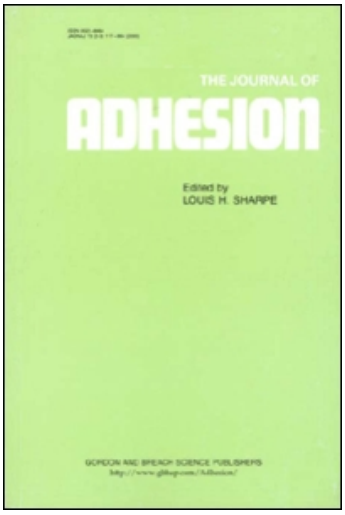

The Journal of Adhesion

Publication details, including instructions for authors and subscription information:
http://www.informaworld.com/smpp/title~content=t713453635

Investigating Fatigue Damage Evolution In Adhesively Bonded Structures Using Backface Strain Measurement

A. D. Crocombe[a]; C. Y. Ong[a]; C. M. Chan[a]; M. M. Abdel Wahab[a]; I. A. Ashcroft[b]
[a] School of Engineering, University of Surrey, Guildford, UK [b] Wolfson School of Mechanical and Manufacturing Engineering, University of Loughborough, Loughborough, UK

Online publication date: 08 September 2010

To cite this Article Crocombe, A. D. , Ong, C. Y. , Chan, C. M. , Wahab, M. M. Abdel and Ashcroft, I. A.(2002) 'Investigating Fatigue Damage Evolution In Adhesively Bonded Structures Using Backface Strain Measurement', The Journal of Adhesion, 78: 9, 745 — 776
To link to this Article: DOI: 10.1080/00218460213835
URL: http://dx.doi.org/10.1080/00218460213835

The Journal of Adhesion, 78: 745–776, 2002

0021-8464/02 $12.00 +.00
DOI:10.1080/00218460290010548

INVESTIGATING FATIGUE DAMAGE EVOLUTION IN ADHESIVELY BONDED STRUCTURES USING BACKFACE STRAIN MEASUREMENT

A. D. Crocombe
C. Y. Ong
C. M. Chan
M. M. Abdel Wahab
School of Engineering, University of Surrey,
Guildford, UK

I. A. Ashcroft
Wolfson School of Mechanical and Manufacturing Engineering,
University of Loughborough, Loughborough, UK

Predicting the service life of adhesive joints under fatigue loading remains a major challenge. A significant part of this task is to develop laws that govern the crack initiation phase. This paper contributes to this area through the development and application of the backface strain technique. A numerical study was carried out to investigate the effect of key parameters on the technique and to determine optimum gauge specification and location. Calibration curves were then produced relating the change in strain to the extent of damage. These numerical studies were then validated by undertaking a series of fatigue tests on both aluminium and GRP (glass-reinforced polymer)-bonded joints. Following various degrees of predicted damage the joints were carefully sectioned, polished, and studied using optical microscopy. The predicted and observed damage showed close correlation. The fatigue tests have also indicated that, for unmodified joints (intact fillets), even at high loads (50% static failure load) there was an initiation phase that accounted for about half the fatigue life of the joint. Removal of the adhesive fillet has been found to eliminate the initiation phase and consequently reduce fatigue life.

Keywords: Fatigue initiation; Backface strain; Bonded joints; Finite Element Analysis; Service life

Received 21 September 2001; in final form 26 April 2002.

The authors are grateful to DERA Farnborough for provision of the joints and to EPSRC, Instron and DERA for support through grant GR/M92263. Thanks also go to Mr. Lenti and Mr. Dron for technical assistance.

Address correspondence to A. D. Crocombe, School of Engineering, University of Surrey, Guildford GU2 7XH, UK. E-mail: a.crocombe@surrey.ac.uk

INTRODUCTION

Adhesive bonding is generally acknowledged to have a fatigue resistance superior to local fastening techniques, such as spot-welding, bolting, and riveting [1]. Nevertheless, it is important to be able to quantify the fatigue performance in order to produce structures that are both safe and efficient. One way of doing this is through the use of empirical laws relating fatigue load to the total life of the structure [2, 3]. A second approach is to divide the fatigue life into crack initiation and crack propagation phases. The propagation phase can be characterized readily using a fracture mechanics approach, such as the Paris law [4–7]. It is much more difficult to quantify the initiation phase and this may be the phase that governs the fatigue life, particularly at low levels of load [8].

Backface strain measurement was first applied to characterize crack initiation and propagation in welded structures [9]. In this technique, a strain gauge is placed on the exposed surface (backface) of the material being joined, near a site of anticipated fatigue damage. This will usually be near the location of load transfer in a joint where the local stresses are high. A number of authors [4, 8, 10] have subsequently applied this technique to adhesively bonded single-lap joints. Zhang et al. [8] carried out experiments with bonded steel substrates and claimed that a peak in the strain indicated fatigue crack initiation. This seems to be rather too broad a statement, as it will be shown that the strain response is very dependent on its location. They did, however, show that the initiation life fraction (Ni/Nf) does increase with decreasing fatigue loads and projected large proportions of life spent in initiation at low loads (i.e., 60% at lives of 10^6 cycles). Imanaka et al. [10] used the technique to compare bonded and hybrid (bonded and riveted) joints and concluded that fatigue cracks in the latter propagated gradually through the fatigue life while in the former the initiation occurred just prior to final fracture. Curley et al. [4] applied backface strain techniques to steel lap joints being fatigued while fully immersed in water. In contrast to the previous two workers, they reported evidence of backface strain changes early in the fatigue life.

None of these three previous papers appear to have considered the effect of the location of the gauge in any detail. However, this paper will show that a small change in location can cause a significant change in the sensitivity of the technique and that careful choice in the location and size of strain gauge will considerably enhance the damage detection. Lefebvre et al. [11] used this technique in the development of a fatigue initiation criterion. However, they used a 3 mm-thick

adhesive wedge bonded to an aluminium cantilever beam at the clamped end. The strain gauge was placed directly on the inclined face of the adhesive wedge near the adhesive-aluminium junction, where fatigue initiation would occur. By selecting different wedge geometries they were able to vary the elastic singularity strength and, hence, to investigate initiation under a wide range of stress fields. The backface strain was used to identify the onset of initiation, and a 3D surface plot showed the variation of initiation life with stress field strength and intensity range. The testing was not continued to final failure and, thus, the relative contribution of initiation to fatigue life was not assessed. The singularity encountered at the point of crack initiation in many bonded joints, included those discussed in this present paper, is of a substrate corner embedded in the adhesive. This singularity was not considered in the work of Lefebvre et al.

Thus, although the role of initiation has not yet been established, a technique for its assessment is available. However, this technique has not yet been used in either an optimal or a quantitative way. The purpose of this paper is to provide a thorough investigation into the backface strain method leading to (1) recommendations for optimal use and (2) validation of damage that is predicted by the strain changes. As a result of this work, some insight is gained into the role of initiation in the fatigue process, but further studies are required to extend this understanding. These studies should include an assessment of the conditions controlling the point of initiation using finite element methods. This could also investigate whether the 3D initiation envelope developed by Lefebvre et al. [11] will extend to more realistic bondline thicknesses and embedded corner singularities.

CONFIGURATIONS AND PROCEDURES

A preliminary experimental study preceded a finite element (FE)-based numerical investigation. This was then followed by the main experimental study. As the configurations involved in both experimental studies were similar, the results will be discussed together and will follow the results of the numerical study.

The basic configuration that is considered in this work is the single-lap joint. This is shown schematically together with the backface strain gauges in Figure 1. Strain gauge length (GL) and centre location (d) are two of the parameters under investigation. The former ranged from 1 to 4 mm while the latter was varied within a zone on either side of the overlap ends. When centred exactly over the overlap end d is equal to zero; d becomes positive as the gauge moves into the

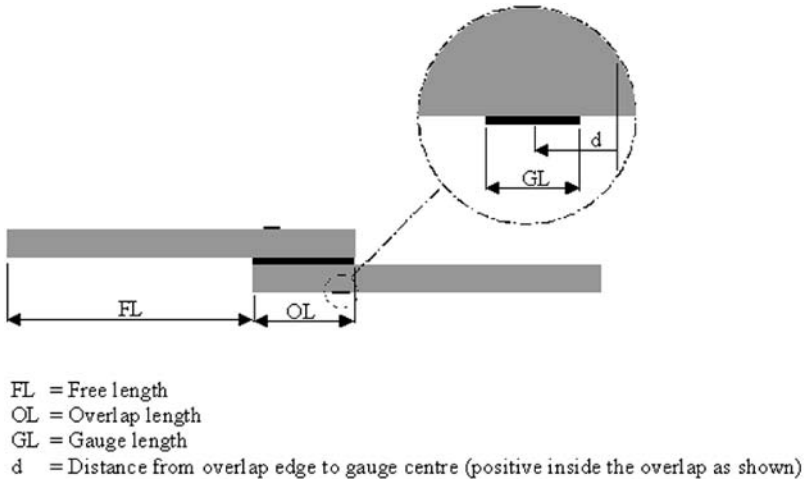

FIGURE 1 Schematic representation of the single-lap joint.

overlap region and negative in the opposite direction, as illustrated in Figure 1.

Three different configurations of lap joint have been investigated. The joint width and substrate thickness were 25 mm and 2 mm in each case, and the other joint parameters are summarized in Table 1. Test configuration 1 (TC1) was used in the preliminary experimental work and consisted of aluminium substrates bonded with a 0.05 mm layer of modified epoxy film adhesive, FM73 (Cytec Ind., N. Peterson, N.J., USA). A total of 10 joints were tested in fatigue, most to destruction. However, backface strain data were only available from a few of these. Test configuration 2 (TC2) formed the larger part of the main experimental study. This was similar to TC1 but was manufactured with a thicker layer (0.2 mm) of the same adhesive. Most of these joints had one of their adhesive fillets removed using a miniature hand file in order to reduce the variability of the fillet shape and to induce failure

TABLE 1 Summarizing the Different Joint Parameters for the Three Configurations of Lap-Joint Tested

	TC1	TC2	TC3
Substrate material	Aluminium	Aluminium	GFRP
Overlap length (OL)	14 mm	12.5 mm	12.5 mm
Free length (FL)	76 mm	102.5 mm	97.5 mm
Adhesive thickness	0.05 mm	0.2 mm	0.23 mm

at a known location. Specific reference will be made to this as the individual joints are discussed. Again, about 10 joints of this configuration were tested in fatigue. Test configuration 3 (TC3) formed the remaining part of the main experimental study and extended investigations into systems with fiber-reinforced polymer composite substrates. Specifically, 16 plies of glass-fiber-reinforced epoxy matrix (GFRP), each 0.125 mm thick, were arranged in $2(0,\pm 45\ 0)_s$ configuration. As the joints were manufactured under a different research programme, the adhesive used was a different modified epoxy film, EA9628 NW (Loctite Corp., Dusseldorf, Germany). One of the adhesive fillets was also removed from some of these joints. The backface strain was recorded from 4 joints in this configuration, although other specimens of this configuration had been tested previously to establish the load-life response.

Fatigue tests of these joints were carried out on an Instron 8511 servo-hydraulic machine. Testing was done in sinusoidal load control at frequencies of 2 or 5 Hz and a load ratio of 0.1. The higher frequency was used after the data logging equipment was updated, in order to accelerate the testing. No frequency effect within this range was noted. The maximum load was varied from test to test and ranged from about 67% to 22% of the static failure load (these correspond with load ranges varying from 60% to 20%, respectively). Maximum and minimum values of load, position, and both backface strains (one on each substrate) were recorded as the test proceeded. This enabled the changes in specimen compliance and backface strain to be established. The latter was used in conjunction with the numerical studies to predict the extent of damage, which was then correlated with experimental observations. It will be seen later that the backface strain changes were an order of magnitude more sensitive than the compliance (position) changes.

Numerical modelling was only carried out on TC2 and TC3 joints as these formed the major part of the experimental programme. A range of two-dimensional, plane-strain finite element models were created. Each of the 16 layers in the composite laminate substrates in TC3 was modelled as a row of elements having the appropriate orthotropic material properties. Typical meshes in the overlap region for both TC2 and TC3 joints are shown in Figure 2, and the material properties used for both substrates and adhesives are summarized in Tables 2 and 3. The fillets in the TC2 specimens varied in shape, and Figure 2a shows two configurations investigated. All fillets in the TC3 specimens were modelled as illustrated in Figure 2b. Where, in the testing, the fillet was removed from one end of the joint, in the FEA model the fillet (shown in Figures 2a and b) was also removed. The effect of cracking

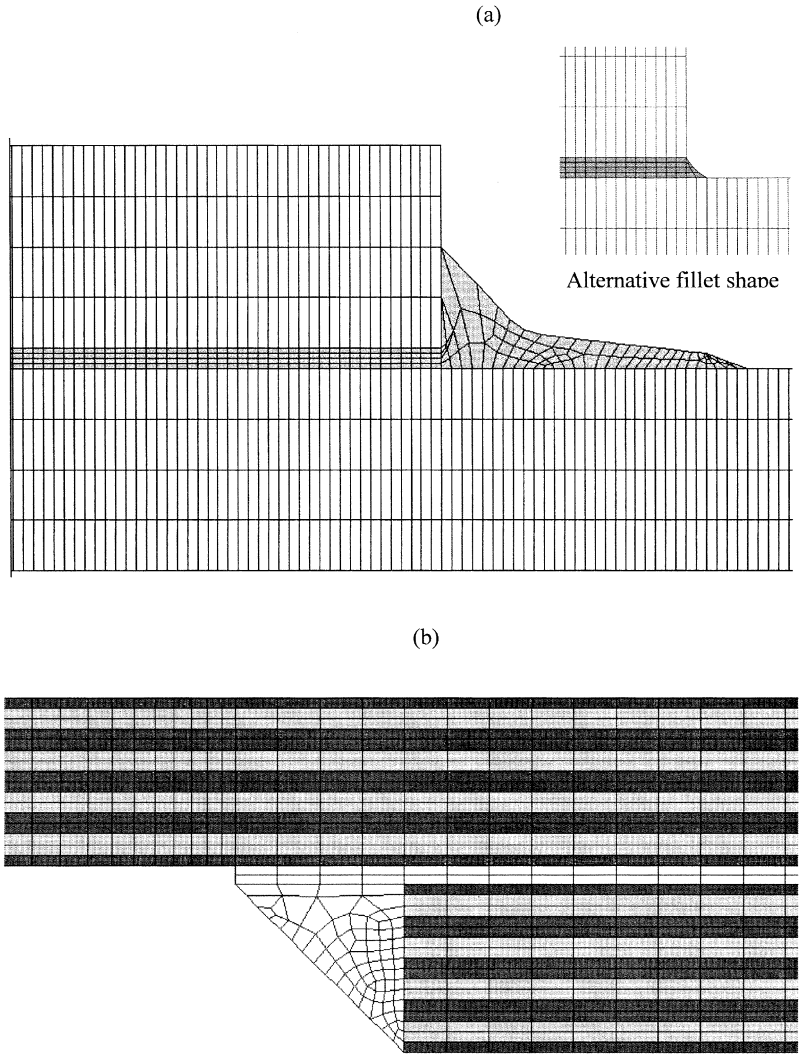

FIGURE 2 Typical FE meshes from (a) TC2 joint and (b) TC3 joint.

in the lap joints was simulated by uncoupling nodes for appropriate distances along the relevant interfaces.

The modelling work was carried out for two main reasons: (1) to undertake a study of the effect of key parameters on the backface strain, and (2) to predict the extent of damage from a knowledge of the

TABLE 2 Isotropic Material Properties Used in Analyses of TC2 And TC3 Joint

	Aluminium	Adhesive TC2	Adhesive TC3
E (GPa)	70.0	2.00	1.90
ν	0.33	0.40	0.38

TABLE 3 Anisotropic Material Properties Used in Analyses of TC3 Joints (Moduli in GPa)

Ex	Ey	νxy	Gxy	Gyz
45.6	10.7	0.3	5.14	4.13

backface strain changes recorded in the fatigue tests. The results from the parametric study will be discussed in the following section, while results related to actual experimental tests will be discussed in the section related to the experimental work.

FINITE ELEMENT INVESTIGATION

Reported here are the results from the analyses that were undertaken to assess the effect of key parameters on the predicted backface strain. The FE code ANSYS was used in this study. These parameters include: (1) geometric nonlinearity, (2) gauge position, (3) gauge length, and (4) substrate material. Each of these 4 aspects will be discussed in turn, identifying their implications on backface strain measurement. It will be seen later in this section that, until the crack has passed significantly beyond the backface strain gauge, the backface strain will be negative. To avoid plotting negative axes in this paper, a compressive backface strain is shown positive.

Geometric Nonlinearity

Although at the level of fatigue loading considered and with the materials used there will be very little material nonlinearity, the rotation encountered by a single-lap joint as it is loaded may cause significant geometric nonlinearity. To assess this, a study was carried out on a model corresponding to the TC2 configuration with no fillets at either end of the overlap. Figure 3 shows the variation of the predicted backface strain with joint loading increasing up to the

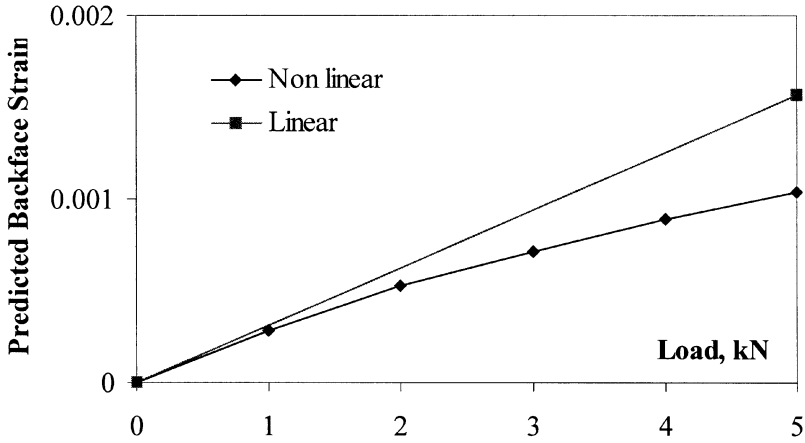

FIGURE 3 Variation of predicted backface strain with load for both linear and nonlinear analyses.

maximum used in the experimental work. The gauge length was set at 1 mm and it was centred 1 mm within the overlap (i.e., d = 1). It will later be shown that these are near optimum settings in terms of measurement sensitivity of the gauges. It can be seen that as the load increases so does the difference between the backface strains predicted by assuming linear and nonlinear behavior. At the maximum load the backface strain evaluated including the nonlinear response is significantly lower (40%) than the value predicted by linear analysis. This is clearly due to the joint rotation reducing the bending moment in the substrate and, hence, the (backface) strains induced. Thus, it can be concluded that it is important to undertake nonlinear analyses in these studies.

A brief investigation was also made into the effect of adhesive yielding. An elastic, perfectly plastic material model with a yield stress of 50 MPa was used for the adhesive. This is a conservative value, based on reported data [12] for FM73, which should overestimate the yielding in the joint. The FE model of the TC2 configuration included fillets, as discussed later, to replicate the actual joint better. At a load of 5 kN the zone of yielded adhesive was of the order of 1–2 mm at each end of the joint. The corresponding change in the backface strain (at d = 1) was less than 1%. Even after increasing the load to 7.5 kN (about 75% of the static failure load), when the yielded zone more than doubled in size the strain only changed by about 5%. A shifting of the strain distribution into the overlap region, as the load transfer was

spread, caused most of this. There was only a 1% reduction in the maximum strain on the substrate backface. Experimentally, once yielding has occurred in the first few load cycles there is unlikely to be any further change in backface strain due to plastic deformation. Creep deformation of the adhesive, if present, may change the strain further with time, but this aspect is beyond the scope of this present investigation.

Gauge Position

To consider the effect of this and other parameters it was necessary to know how the backface strain changed with increasing fatigue damage. This was modelled as an evolving fatigue crack. These data were built up by carrying out a series of analyses with increasing crack lengths. By selecting a fixed point on the substrate (or averaging over a fixed zone representing the gauge length) and considering the strain for each of the analyses (i.e., as the crack length increases) it was possible to obtain the predicted variation of backface strain with crack length. From this it was possible to determine optimum conditions for detection of small levels of damage corresponding to fatigue crack initiation. Shown in Figure 4 are the strain distributions along the substrate backface for a range of crack lengths, propagating only from the nonfilleted end of a joint, corresponding to the TC2 configuration, loaded to 4 kN. As the crack length (a) grows, the position of the strain peak moves to the right. It is necessary to distinguish between the substrate whose loaded portion is adjacent to the crack (S1) and the substrate whose free end is adjacent to the crack (S2), as illustrated in Figure 4. The backface strains of substrate S1 are shown in Figure 4. The horizontal axis represents distance into the overlap from the lefthand end (note that the overlap length is 12.5 mm). Geometric nonlinearity has been included in these analyses. It is instructive to consider these distributions before investigating the effect of gauge position and length as a number of important points emerge.

Consider first the results from the uncracked model ($a = 0$). It can be seen that the substrate strain is maximum a short distance (about 0.5 mm) outside the overlap region. Although the actual position changes slightly, the maximum backface strain has always been observed to occur just outside the overlap for the wide range of joint parameters considered in this work. This is because the load transfer from the loaded to the unloaded substrate begins around this point. Where a regular fillet has been modelled the maximum occurs just outside the toe of the fillet, at a slightly smaller distance than in the nonfilleted case. The point of load transfer, and, hence, the location of

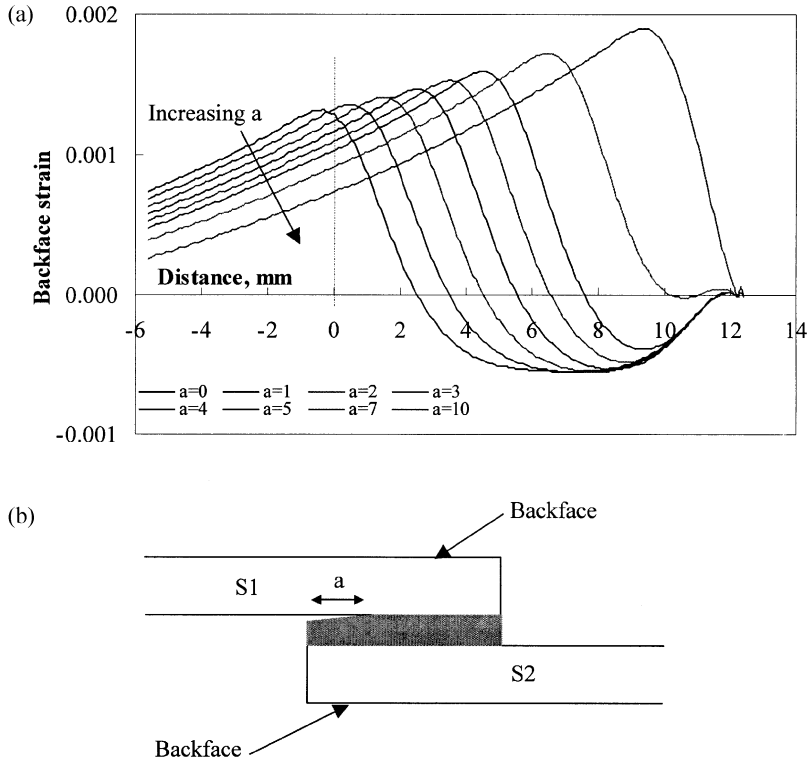

FIGURE 4 Substrate (S1) backface strain distribution for various crack lengths (a).

the peak in the backface strain, moves with the crack tip, always remaining a short distance outside the remnant bonded region. The other point to note is that the magnitude of the backface strain peak also increases with increasing crack length. The axial loading in the substrate does not change at 4 kN, and thus this increase in strain must come from an increase in bending moment that occurs as the free length of the substrate increases. This was confirmed by another analysis where the free length was increased and the (uncracked) overlap length remained fixed. It was found that the substrate strains increased with the free substrate length.

When the same analyses were carried out under small displacement (linear) assumptions it was found that, while the increase in the strain peak still occurred, it was less pronounced, and the parts of the curves in Figure 4, which were obtained from the unbonded substrate,

were much more closely packed together. This would be expected because, as the free length was increased, the effect on joint rotation was enhanced and this was only picked up in the geometric nonlinear analyses. This also caused the larger increases in backface strain peak with crack length. A final observation from Figure 4 is that the backface strains all tend to zero at the righthand end of the overlap as this is a free surface which can transmit no axial stress.

At this stage it is worth commenting on the corresponding strain distribution from the other substrate, S2. These distributions are shown in Figure 5. As anticipated, there is no major shift in the location of the peak stress as the crack grows (at the other end). It actually can be seen to move a small distance further away from the overlap end. However, the magnitude of the strain peak increases with increasing crack length. This is because as the crack grew the joint became more asymmetric, a larger moment was induced in this substrate, and the location of the moment shifted away from the overlap slightly. The location of the peak lies further outside the overlap region as the model included a larger irregular fillet at this end of the joint.

Models have also been analyzed for cracking that occurred simultaneously at both ends of the joint. Under these conditions the symmetry is retained and both gauges had the same output, which was similar to that shown in Figure 4. However, because there was no increase in moment due to asymmetry, the increase in strain with crack length was somewhat less than shown in Figure 4 and the

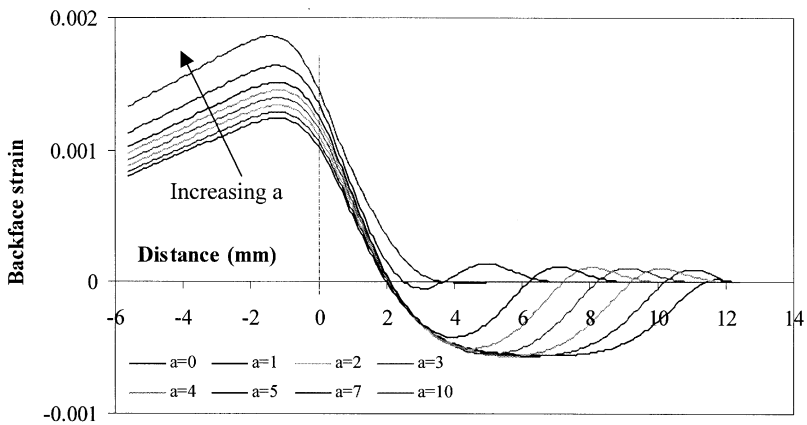

FIGURE 5 Substrate (S2) backface strain distribution for various crack lengths (a).

strains in the unbonded part of the substrates followed a single curve which did not change as the crack grew.

With these observations made, the effect of crack length on backface strain can be assessed as follows. Consider first the situation when the damage occurs only at one end of the joint. As this damage grows, Figure 5 indicates that the backface strain measured on S2 will grow slightly, irrespective of the actual location of the gauge (within reason). However, the change in backface strain measured on S1 will depend on where the gauge is located. If it is centred more than about 0.5 mm outside the overlap, then Figure 4 indicates that as the crack grows the strain will gradually decrease. However, if it were placed a small distance inside the overlap there would initially be a more rapid increase in strain as the load transfer point approached the gauge, followed by a more gradual decrease. These points are elegantly summarized in Figure 6, which shows the variation in predicted

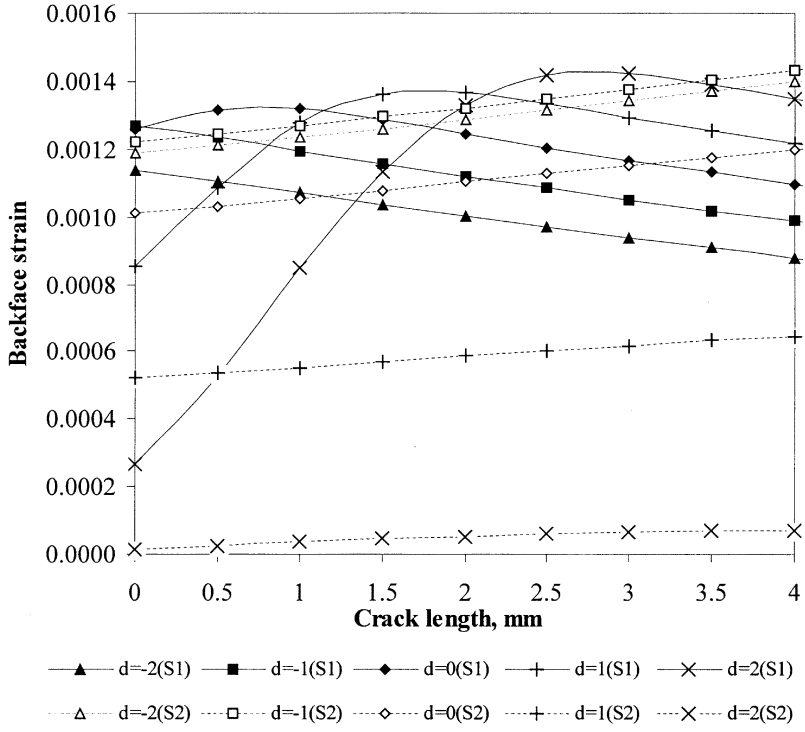

FIGURE 6 Variation in backface strain with crack length for various gauge locations.

backface strain (gauge length 1 mm with damage evolution (at only one end of the joint) at 4 different gauge locations on both S1 and S2. The backface strains on S2 (dashed lines) all show a gradual increase with crack length. However, on S1 (solid lines), those gauges placed just within the overlap (d = 1 or 2) show a more rapid increase before a slower decrease. To maximize the sensitivity of this technique in detecting fatigue crack initiation (small crack lengths) it is necessary to use the gauges where they exhibit maximum change in strain with crack length. Thus, it is appropriate to place them about 1 or 2 mm within the overlap region. The previous users of this technique [8, 10, 11], cited in an earlier section, do not seem to have adopted this approach and thus may not have used this technique to its full advantage. Another important reason for positioning the gauge within the overlap is that it is then possible to observe the peak in the backface strain, and this in turn enables an estimate of the extent of damage within a joint to be made without having to run FE simulations. Knowing that the peak occurs a small distance (say 0.5 mm in front of the crack (damage) tip, if a gauge is then placed x mm into the overlap when the peak is observed the damage should have extended about $x + 0.5$ mm into the joint. It will be seen in experimental work reported in a later section that this is quite an accurate approximation.

If cracking occurs at both ends of the joint simultaneously and the gauges are placed a small distance within the overlap, the strains will be as in d = 1 or 2 (S1) in Figure 6, but based on earlier observations the strain increases will be smaller and the downturn following the peak will be negligible. The response for different proportions of cracking at each end can be estimated by judicious combination of these results. This will be illustrated when the experimental results are considered later in this paper.

Gauge Length

The data presented in Figures 4 and 5 can be reprocessed in a similar way to the results shown in Figure 6, but with averaging over larger zone sizes to give the results for larger lengths of strain gauges. This has been done, and the results are presented in Figure 7 for different gauge lengths centred 1 mm within the overlap on the S1 substrate. It can be seen that a longer gauge length appears to make the technique slightly less sensitive (i.e., lower slope of the strain-crack length curve). This is because the strains are averaged over a larger region and this damps out the strain changes. Thus, it is appropriate to use as small a strain gauge as possible. This, however, must be balanced

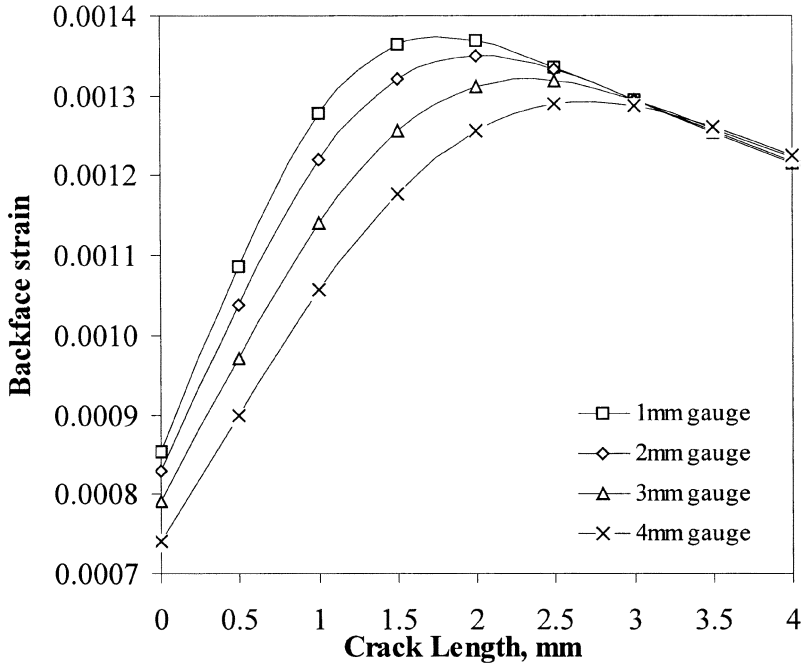

FIGURE 7 Variation of backface strain with damage growth for various sized gauges.

against the increased difficulty of installing small gauges and a suitable compromise reached.

Substrate Material

A final aspect of this parametric study is to consider the effect of the substrate material. In addition to the two substrates used in TC2 and TC3, a third material has been included in the modelling work. This is a carbon-fiber-reinforced polymer, a natural complement to the glass-fiber-reinforced polymer considered in TC3. In fact, the same FE model has been used but the material properties cited in Table 3 were replaced with those given in Table 4. Also presented are the results from a TC3 joint with a regular fillet.

Sets of analyses were run for the four configurations for a load of 4 kN and a range of crack lengths. The results were processed as outlined above. A gauge length of 1 mm centred 1 mm within the overlap has been considered. It will be seen, by comparing the data

TABLE 4 Anisotropic Material Properties of Carbon-Fiber-Reinforced Polymer (Moduli in GPa)

Ex	Ey	νxy	Gxy	Gyz
137.0	8.9	0.3	5	3.4

in Table 2, that, apart from the substrate material, the TC2 and TC3 joints do not differ significantly. The latter has a slightly lower free substrate length but a slightly greater adhesive thickness. To a certain extent, these effects cancel out and it is felt that they will not significantly alter the substrate backface strains. The results for the different configurations are presented in Figure 8. From this, a number of observations can be made. As expected, the value of the peak strain increases with the flexibility of the substrate, with the most flexible (GFRP) having the highest backface strain values. Also the "sharpness" of the strain peak appears to be greatest for the most

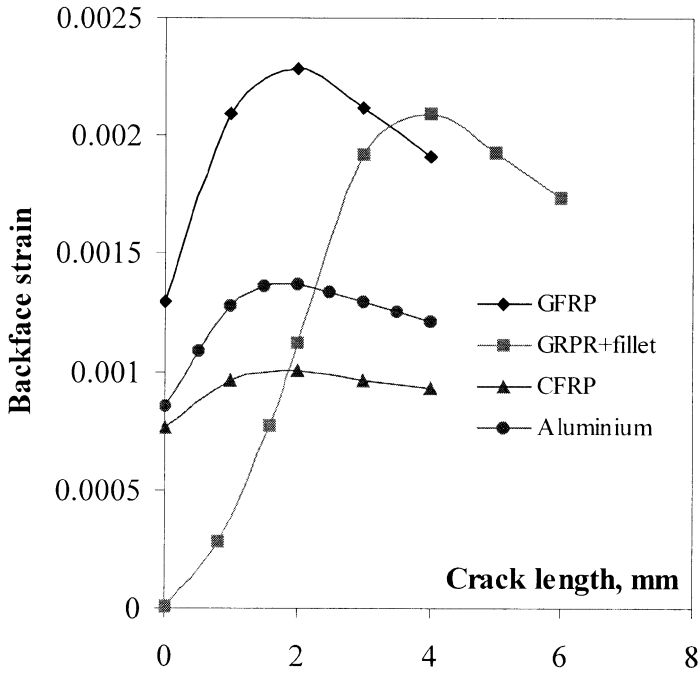

FIGURE 8 Variation of backface strain with fatigue crack length for different substrate materials.

flexible substrates. This is related to the intensity of load transfer within the joint. Basic joint mechanics [13] indicate that the zone over which load transfer takes place within the overlap is proportional to Et_1t_3/G, where G is the adhesive shear modulus, E the substrate tensile modulus, and t_1 and t_3 are the substrate and adhesive thicknesses respectively. The smaller the load transfer zone the sharper the backface strain peak, and thus it can be seen that for a given adhesive bondline a more flexible substrate (low Et_1) will result in a smaller load transfer zone and, hence, a sharper backface strain peak.

Another observation is that the position of the strain peak appears to be largely unaffected by the substrate material. In Figure 8 the crack length is measured either from the overlap end or the toe of the fillet (if one exists). For the filleted joint it can be seen that the peak is simply shifted by the length of the fillet (2 mm), and thus it occurs when the crack tip is at the same point relative to the overlap end. Finally, the presence of a fillet appears to reduce the peak value of the backface strain somewhat. This is probably not due to the fillet where the crack is propagating but to the fillet at the other end of the joint which affects the symmetry in such a way as to reduce the strain at the other end of the joint (the opposite of a crack at one end increasing the strain at the other end, i.e., S2 in Figure 6).

FATIGUE TESTING OF ADHESIVE JOINTS

The principal aims of this experimental work are: (1) to validate the FE results for backface strain, (2) to validate the damage predictions based on measured backface strain changes, and (3) to generate useful fatigue data which can be used as a basis for further work. In addition to the backface strain measurements, in situ video microscopy was also used to identify cracking. A series of static and fatigue tests were undertaken and are reported separately below. There was some variation in the specimen geometries, and to accommodate this in any supporting analysis work individual FE models were often created.

Preliminary Work and Static Testing

The accuracy of the gauges and instrumentation were assessed before and after the fatigue-testing program, by undertaking a tensile test of steel. The measured strains were used to calculate the tensile modulus. The correct value was found, both before and after the test program, thus establishing the accuracy of the strain-measuring system. Based on the results of the analysis it was anticipated that the backface strain would change as fatigue damage occurred. It is

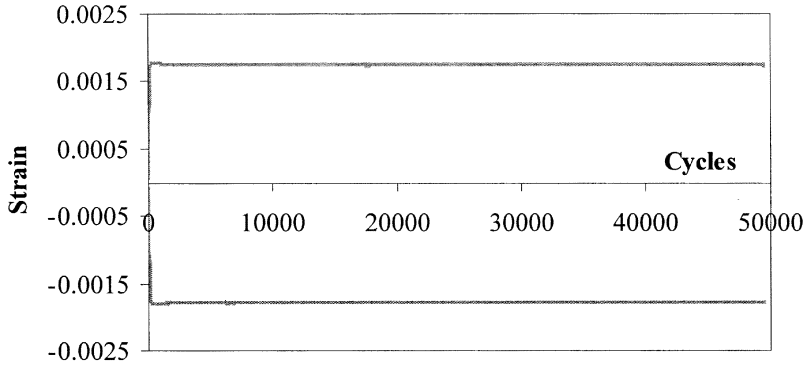

FIGURE 9 Strain gauge integrity tests carried out in four-point bending.

necessary to ensure that this is due to cracking within the joint and not to a loss of integrity of the strain gauge or its bond to the substrate. This was established by attaching strain gauges to the top and bottom surfaces of a 4-point bend specimen made from the same aluminum as the substrates. This was then tested in fatigue, with the gauges experiencing a similar magnitude of strain to that encountered in the fatigue tests. Figure 9 shows the variation of mean strain with the number of cycles for the top gauge (tensile) and bottom gauge (compression). It can be seen that there was no observable change in maximum and minimum strains over the 50,000 cycle duration of the test. It was thus concluded that the integrity of the strain gauging is acceptable.

Static testing, at a crosshead speed of 1 mm/min, was carried out to determine the ultimate static strength of the joints. The results for the three test configurations are given in Table 5. Some of the TC2 fatigue specimens were first loaded statically in order to assess the accuracy of the backface strains predicted by the FE analysis. Figure 10 shows the comparison between measured and predicted backface strain for one such test. In this specimen the strain gauges are placed about 1 mm within the overlap region. The good correlation that can be seen establishes the accuracy of the strains predicted by the FE method.

TABLE 5 Summary of the Static Strength of the Three Test Configurations

TC1	TC2	TC3
10.2 kN	10.0 kN	12.6 kN

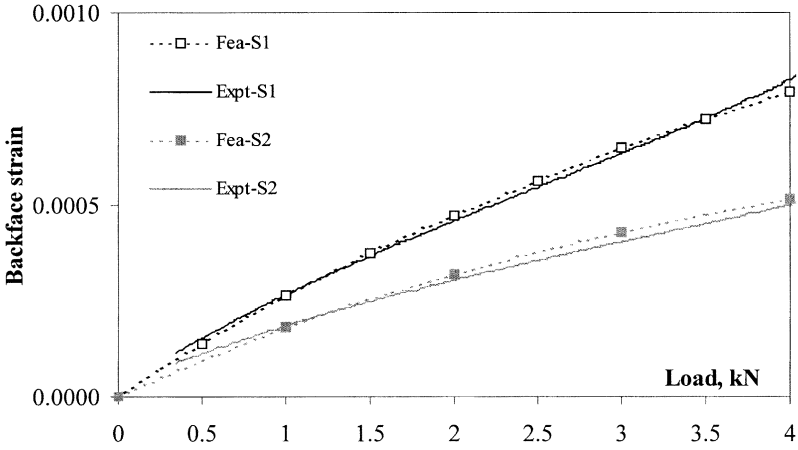

FIGURE 10 Comparison of the measured and predicted backface strains for a TC2 specimen loaded statically to 4 kN.

Note that the strain on one substrate (S1) is significantly higher than that on the other (S2). This is a result of the adhesive fillet adjacent to the S1 gauge being removed. The load transfer point is then shifted more towards the overlap and the S1 gauge, which is placed within the overlap, experiences a corresponding increase in strain.

Fatigue Testing

The results from the fatigue tests will be discussed separately for the three test configurations under consideration.

TC1 Joints

These joints were fatigued at a frequency of 2 Hz in load control at a load ratio of 0.1. Most of these joints were fatigued to failure in order to establish a load-life response curve. The relationship between the fatigue load range (ΔP), normalized by the static failure load (P_s), and the cycles to failure can be seen in Figure 11. This appears to correlate well with load-life data obtained for other joint configurations using other material systems [2].

As well as obtaining a load-life response curve, the TC1 specimen tests were used to develop the backface strain measurement methodology. For this reason, only a limited amount of backface strain data was obtained. Figure 12 shows data from one of the later TC1 specimens to be tested. Similar plots were found for a number of these

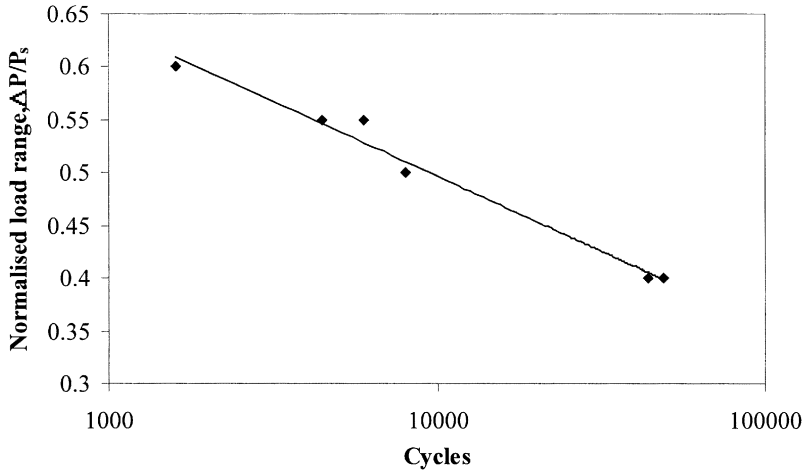

FIGURE 11 Load-life data obtained for TC1 joints.

later specimens. The data being shown are both backface strain ranges and the actuator position range. The strain gauges were positioned outside the overlap (i.e., non-optimally) and the fatigue load range was maintained constant at 40% of the static failure load. At this

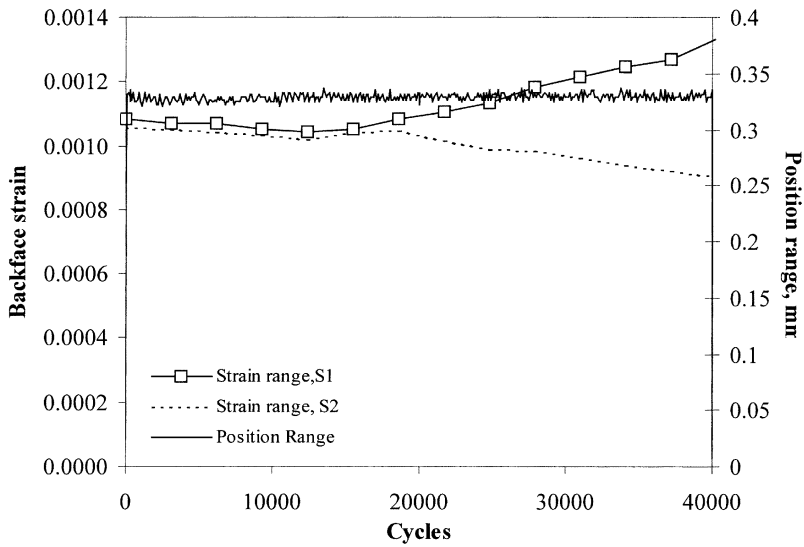

FIGURE 12 Typical backface strain and position ranges for a TC1 joint.

load, based on Figure 11, one would expect a total fatigue life of around 45–50,000 cycles. A number of observations can be made from this figure. Initially, both backface strains show similar, essentially constant values. The initial similar values would be expected as both adhesive fillets had been retained in this joint, resulting in a symmetric strain distribution. The period of unchanging (essentially constant) strain suggests that no damage occurred over the first half of the fatigue life. At about 20,000 cycles there is evidence of the strains separating which suggests the onset of damage evolution. The growing disparity in the strains indicates that the damage continued to evolve. In this configuration the gauges were placed outside the overlap and thus, from Figure 6 ($d = -1$), the strain evolution is consistent with damage occurring primarily at one end. It is also worth noting that during the whole of this test the compliance (actuator position) gives no indication of the damage that is evolving. This clearly suggests that backface strain is a much more sensitive technique than compliance. Having said this, significant damage would be expected towards the end of the test but the changes seen in the backface strains are quite modest. It is possible that damage could be occurring even earlier but is not being picked up by the strain gauges. This then provides a good reason for moving the strain gauges to a more optimal position, enhancing the sensitivity of the technique still further. As a final observation it can be seen that even at these relatively high levels of fatigue load (relatively short fatigue lives) the initiation of damage seems to account for about 50% of the life of the joint. Based on the comments of other researchers [8] and work reported elsewhere [2] one would expect this proportion to increase further as the level of fatigue loading is reduced.

TC2 Joints

With the preliminary study completed, the analytical investigation was undertaken to enhance understanding of the technique. These TC2 joints were then tested to validate some of the key findings of the analytical investigation, including: (1) the optimal location of the gauges and (2) the accuracy of the predicted extent of damage. As with TC1, fatigue testing was carried out in load control at a load ratio of 0.1 and at a frequency of 2 Hz.

Figure 13 shows the evolution of backface strains from two tests. In one, the gauges were placed 1 mm outside the overlap end ($d = -1$) while in the other they were placed 1 mm within the overlap ($d = 1$), a position that FE analysis indicated would give a much-enhanced sensitivity. A constant load range (ΔP) of 5 kN was used. Although the adhesive thickness is greater in TC2 joints, the load life data in

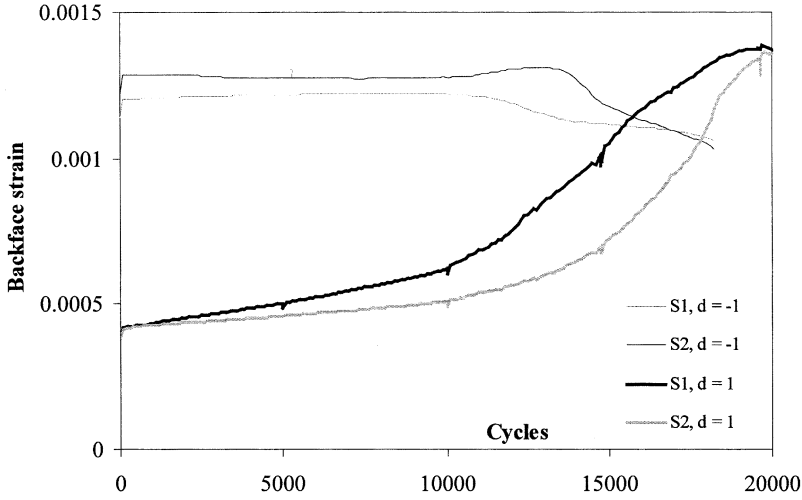

FIGURE 13 Backface strain range data for TC2 joints with gauges (a) 1 mm outside the overlap (d = –1) and (b) 1 mm within the overlap (d = 1).

Figure 11 would still suggest that this load range would give quite a short fatigue life. This can be seen to be the case from the actual data shown in Figure 13, where it is evident that the two joints failed at about 18,000 and 20,000 cycles, respectively. The fillets in both joints were not removed prior to testing. In both joints there is an indication of major damage evolution at about 10,000 cycles. However, as suggested by the FE study, the changes in backface strain are much more apparent in the specimen with gauges within the overlap (d = 1).

Consider first the specimen with gauges outside the overlap (d = –1). There is little evidence of any damage until about 10,000 cycles; at this point there is a small increase in the strain on one substrate (S2) and a corresponding decrease in strain on the other substrate (S1). With reference to Figure 6 (d = –1), damage evolution occurring at the S1 end of the overlap could cause this response. A possible reason for the damage occurring first at S1 is that the fillet was noticeably smaller (and, hence, more prone to damage) at this end of the overlap. However, after a few thousand more cycles the strain at S2 begins to decrease and the rate of reduction in strain at S1 lessens. This could be caused by additional damage now occurring at the S2 end of the joint as well. However, as with the data in Figure 12, the strain changes are small compared with the strain signal and it is difficult to draw firm conclusions.

Turning now to the other specimen, it can be seen that repositioning the gauges significantly enhanced the changes in the backface strain.

A comparison of both specimens indicates that there was considerably more asymmetry in the failure surface of this latter specimen. Thus, the initial increase in backface strain, which is not evident in the previous specimen, may be due to misalignment in the loading train. Whatever the cause, the initial backface strain evolution, considered in conjunction with Figure 6 ($d = 1$), suggests that the damage may have accumulated at S1 as the gradient is steeper there (compare the gradients of the solid and dashed lines for $d = 1$ in Figure 6). However, an abrupt increase in this rate of damage evolution can be seen just after about 10,000 cycles. Towards 15,000 cycles the gradient of the backface strain on S2 increases and ultimately exceeds that on S1. This suggests that, at this point in the test, damage also built up on the S2 face. Towards the end of the fatigue life the backface strain curves appear to reach a peak. This could correspond with the strain peaks seen in Figure 6 and, if so, would indicate that, by this stage, the damage in the adhesive had passed the point adjacent to the backface strain gauge and was about 0.75 mm in front of the gauge.

To investigate the accuracy of these predictions of the extent of damage, further specimens were tested with strain gauges positioned 1 mm inside the overlap ($d = 1$) with a reduced load range of 4 kN. These tests, however, were halted after the accumulation of a certain amount of backface strain (damage). These specimens were then sectioned, polished, and inspected using reasonably high magnification light microscopy to ascertain the actual extent of damage. In an attempt to control the location of fatigue damage accumulation, the adhesive fillet was removed from one end of the joint in these specimens. The evolution of the backface strain for one such test is shown in Figure 14, where it can be seen that the test was halted after about 10,000 cycles. In comparison with Figure 13 it can be seen that the backface strains increased at a much higher rate, indicating a more rapid evolution of damage. This can probably be attributed to the damage that was generated when removing the adhesive fillet. The strain on S1 is higher than that on S2, as the adhesive fillet was removed from the S1 end of the joint. Comparing the two curves corresponding to $d = 1$ on Figure 6, the data in Figure 14 are entirely consistent with damage growing from the S1 end. As this is the end from which the fillet was removed, this seems entirely appropriate. Over the period of testing the strain has increased by nearly 0.0003, and from the rising curves on Figure 6 this increase should correspond to a crack length of around 0.75 mm.

The joint was removed from the testing machine and three sections were made, mounted, and polished. The locations of the sections are shown in Figure 15 and lie on the centreline, midway between the

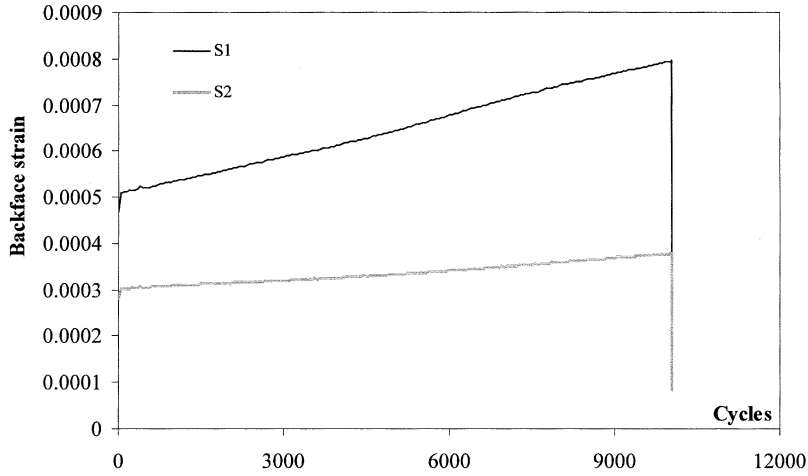

FIGURE 14 Variation of backface strain range with fatigue cycles.

centreline and the edge, and near the edge. Figure 16 contains a series of images from the centreline section at the S1 end of the joint. It is clear from these that the observable damage appears to extend about 0.75 mm as predicted. It is also clear that the damage was distributed

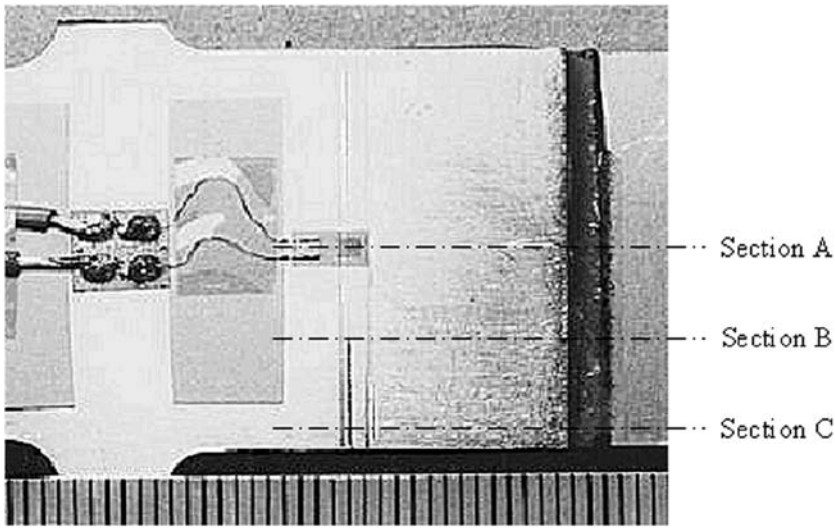

FIGURE 15 Photo showing the locations of the sections cut from the test specimen.

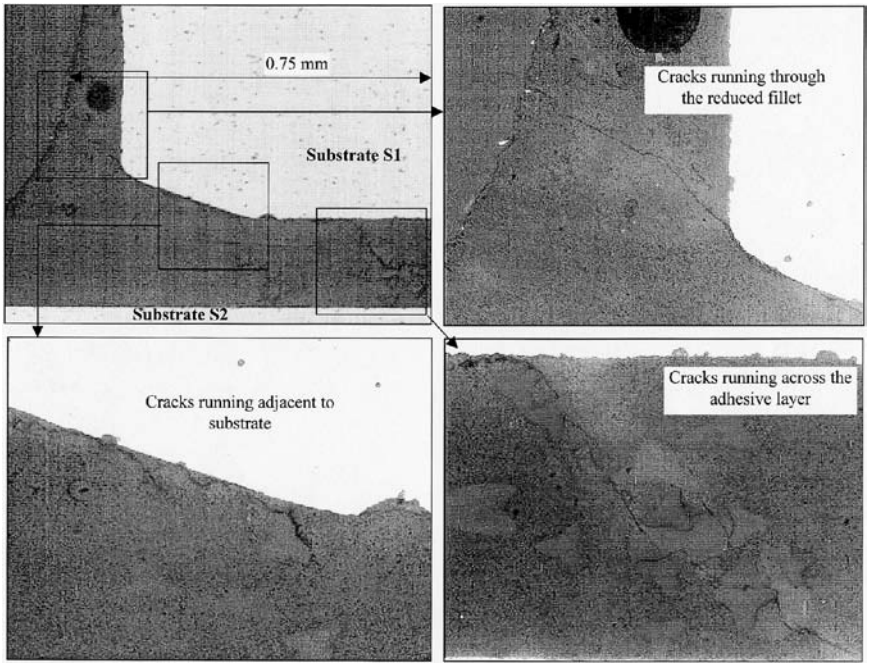

FIGURE 16 Images of the centreline section (Section A) showing extent of fatigue damage.

rather than forming as a single through-width crack. On this section the damage appears to run through the reduced fillet, adjacent to the substrate and then across the adhesive thickness to the lower substrate. It can also be seen that the polyester carrier mat, used by this adhesive, influenced the crack path at a local level. Similar studies on the other sections show that the extent of damage appears to reduce towards the edge of the joint, measuring about 0.45 mm and 0.35 mm, respectively. Other specimens were tested in a similar manner and the damage found on the polished sections was broadly consistent with the data discussed and illustrated here.

From Figure 14, and data from similar tests, it would appear that (unlike TC1 and early TC2 specimens) fatigue damage accumulated from the onset of the test. This can be attributed to the removal of the adhesive fillet, which occured in these later joints. In order to investigate the effect of fatigue load level, tests were carried out at various load ranges. The backface strain data for one such test are shown in Figure 17. Testing was carried out with an initial load range

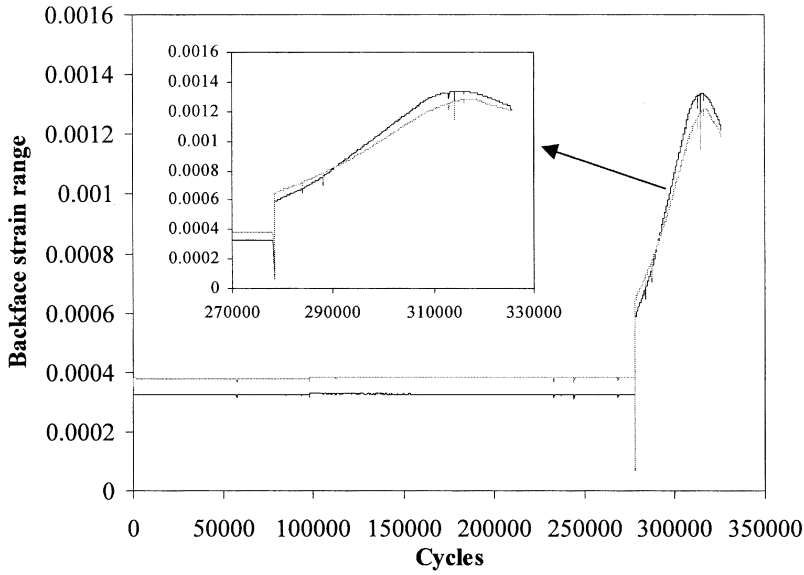

FIGURE 17 Variation of backface strain range with fatigue cycles for stepped loading.

of 2 kN, which was raised to 4 kN after about 270,000 cycles. It can be seen that while the load range is at 2 kN there is no evidence of any fatigue damage. Both adhesive fillets were removed from this specimen and the small difference in S1 and S2 backface strains is attributable to slightly different positions of the strain gauges (positioned nominally 1 mm within the overlap). This, then, suggests that there is a limit below which even the microcracks, induced in removing the adhesive fillets, will not propagate.

When the load range increased to 4 kN, both backface strains began to increase. The similarity in the strain traces suggests that damage accumulated essentially in equal measure from both ends of the overlap (consistent with the removal of the adhesive fillets from both ends of the overlap). There is clear evidence of the peak, and subsequent downturn, in the backface strain, which has been shown to occur as the damage extends beyond about 0.75 mm past the gauge. This would suggest that final failure occurred when the fatigue damage extended to about 2 mm on either end of the joint. This is very consistent with the failed surface, which shows a different topography a few mm in from both ends of the overlap. It is also encouraging to note that the strain distributions are quite consistent,

in shape and magnitude, with the FE data shown as a solid line (d = 1) in Figure 6.

TC3 Joints

Previous fatigue testing [14] undertaken in load control at a frequency of 5 Hz and a load ratio of 0.1 has established the load-life response for these joints, shown in Figure 18. Backface strain gauges were applied to some of these joints and tests were undertaken to investigate the evolution of damage in these GRP substrate joints. To be consistent with the TC2 testing, the adhesive fillets were retained in a first set of joints tested while one fillet was removed in a second set of joints. All tests in both sets were carried out in load control at a frequency of 5 Hz and a load ratio of 0.1.

The first set of joints were all fatigued at a maximum load of 3.75 kN. Based on Figure 18 and Table 5 this should provide a fatigue life of about 50,000 cycles. Similar patterns of backface strain evolution were obtained from all joints and a typical set is shown in Figure 19. In this joint, backface strain gauges 5 mm long were used, centred on the overlap end (i.e., d = 0). The joint failed at around 48,600 cycles, this being very consistent with the anticipated life at this level of fatigue load. The evolution of damage seems to be similar to the fully filleted TC1 and TC2 joints (Figures 12 and 13). There is a period of about half the fatigue life (up to about 25,000 cycles) where there is no discernable damage (change in backface strain). This could be termed the initiation phase. It appears that then damage accu-

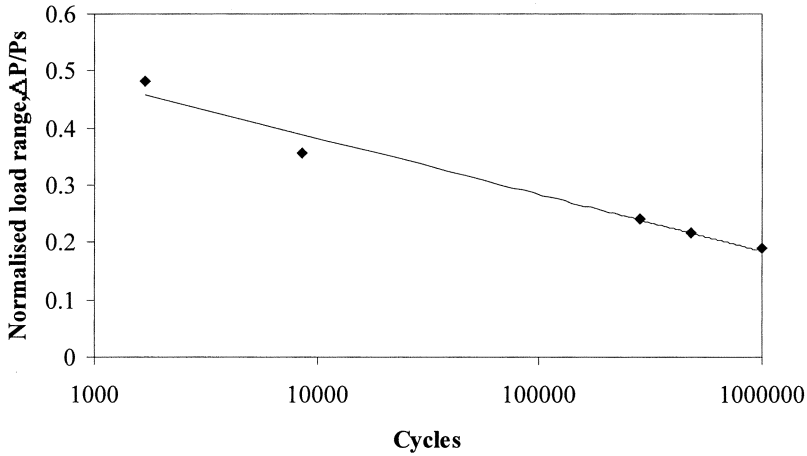

FIGURE 18 Load-life data for the TC3 joints.

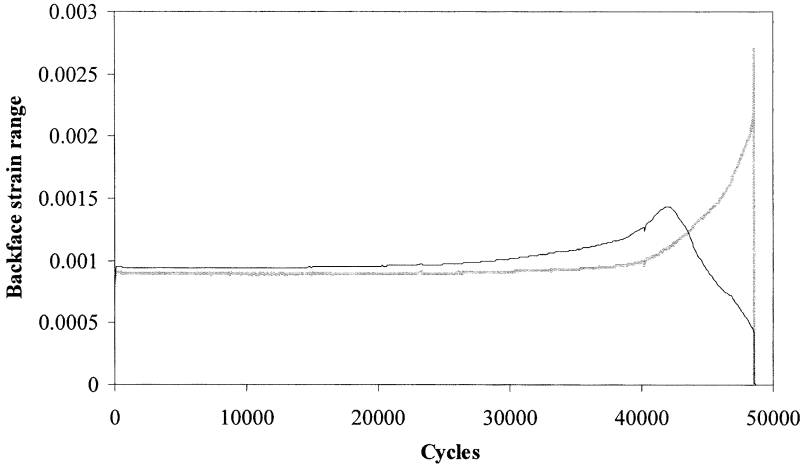

FIGURE 19 Variation of backface strain with fatigue cycles for a full-filleted TC3 joint.

mulated at one end of the joint (where the steeper increase in strain occurs). Based on the trends shown in Figure 7, the peak in this strain indicates that the damage had spread as much as a few millimeters from one end of the overlap. The decreasing strain indicates that this growth continued in a stable mode. The other strain continues to increase and does not peak. This would suggest that damage at this end of the joint did not extend far. The increase in strain is obtained from a combination of the asymmetry caused by crack growth at the other end (as in the S2 curves in Figure 6) and some limited damage at its own end (as in S1 curves $d = 0$ in Figure 6). The failure surface, which shows failure to have occurred entirely adjacent to one interface (just within the adhesive), supports this scenario. The value of the strain peak in Figure 19 is reasonably consistent with data shown in Figure 8 after considering the following factors: (1) the load used to generate Figure 8 was 4 kN, while the test was carried out at 3.75 kN; (2) the gauge length used in Figure 8 was 1 mm, while that used in the TC3 tests was 5 mm (Figure 7 shows how a larger gauge results in a lower strain); and (3) Figure 8 presents maximum strain, while Figure 19 presents strain range.

The last set of joints tested had one of the adhesive fillets removed. In an attempt to achieve a similar sort of fatigue life the maximum load was reduced to 3 kN. The backface strain range evolution for one specimen with gauges of length 1 mm positioned 1 mm within the

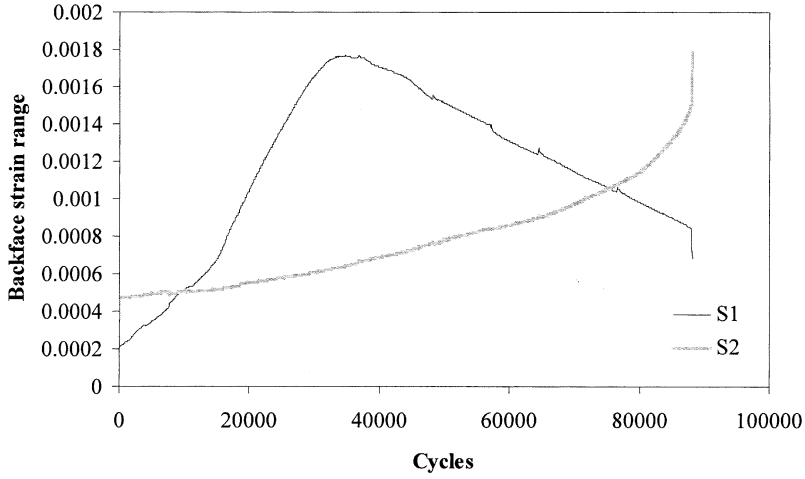

FIGURE 20 Variation of backface strain range with cycles for a TC3 joint with one fillet removed.

overlap is shown in Figure 20. The S1 gauge was at the end of the overlap where the fillet had been removed. The strains are lower here initially as the gauge was set a little further within the overlap than at the other end where the fillet was not removed. It is clear that the damage accumulated faster at the S1 end of the joint. In many ways this is similar to the fully filleted joint shown in Figure 19. One strain rises to a peak and falls while the other only rises and with a gradient that is initially lower than the first gauge. Thus, the same failure mode, of crack formation and propagation principally from one end, would seem to apply. Final failure occurred at just over 88,000 cycles. The main difference between Figures 19 and 20 is that there is no "initiation" period, where the backface strains remain essentially unchanged. Thus, as with TC2 joints, it would seem that the removal of a fillet introduces microcracking and damage, that results in immediate damage growth. Although tested at a lower load the strain peak is higher in Figure 20. This is because a much smaller length strain gauge was used, and from Figure 7 it can be seen that this will generate a higher backface strain signal.

The last specimen in this set was tested under a series of multilevel loads. Initially a maximum load of 2.9 kN was applied for 50,000 cycles, which ensured that a reasonable degree of damage had accumulated at both ends of the joint, with more occurring at the end where the fillet had been removed. The backface strain evolution over

the 50,000 cycles at 2.9 kN was similar to that shown in Figure 20 (3 kN) over the initial 20,000 cycles. Following this the maximum load was reduced to 1 kN and gradually stepped up, undertaking a few tens of thousands of cycles at each load level. At each load level the rate of change of strain with cycles was determined. These data are shown in Figure 21 where it can be seen that below a maximum fatigue load of about 2kN there is essentially no change of backface strain. Although only a preliminary test, this appears to offer a very convenient way of identifying a threshold fatigue load, below which the damage evolution is negligibly small. In this joint, the gauge S2 was at the end of the overlap where the fillet was removed. Although during the preliminary testing at 2.9 kN more damage occurred at the S2 end, by the end of the test the rate of damage generation (strain increase) was higher at the S1 end. This trend is continued throughout the subsequent testing, and Figure 21 shows that the crack growth rates at end S1 are higher than those at end S2.

In fact, it is possible, using these data in conjunction with the FE analyses, to determine the crack propagation rate (da/dN) corresponding to the backface strain gradient. Based on the FE analyses of the TC3 joints, an approximate conversion of the backface strain

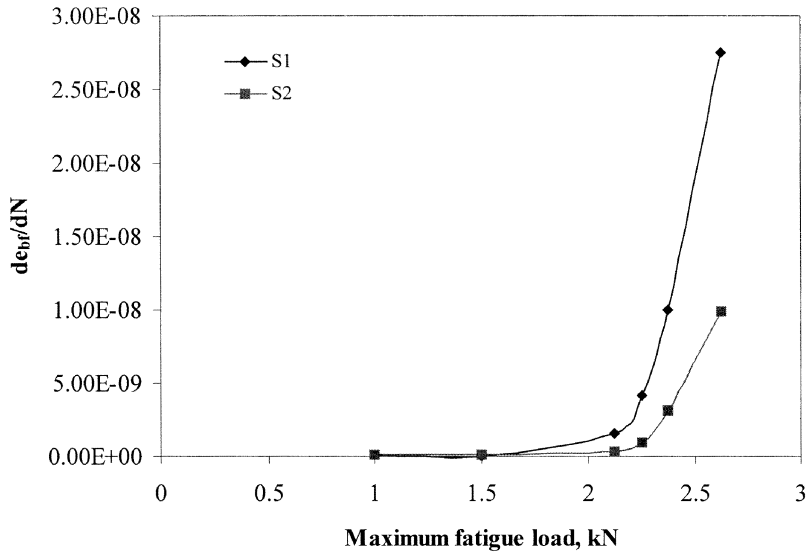

FIGURE 21 Variation of backface strain gradient ($d_{\varepsilon_{bf}}/dN$) with maximum fatigue load level.

gradient to the crack propagation rate in the region where the back-face strain is rising can be expressed, for an applied load P, as

$$\frac{da}{dN} = kP\frac{d\varepsilon_{bf}}{dN}$$

where

$$k = 352\,\text{mm}/kN\,\frac{\text{mm}}{\text{mm}}.$$

This provides a very convenient way of measuring the crack propagation rate, which can be used even when a crack is not clearly visible. These crack propagation rates should be a power law function of the energy release rate, expressed as the Paris law. The energy release rate is proportional to the square of the load, and thus the crack propagation rate should also be a power law function of the load. To check the validity of the crack propagation rate, and to demonstrate how this technique can be used to determine the Paris law, the crack propagation rate has been plotted against the load in Figure 22. Also shown in this figure are the best-fit power law curves. It can be seen that the data are a good fit to a power law.

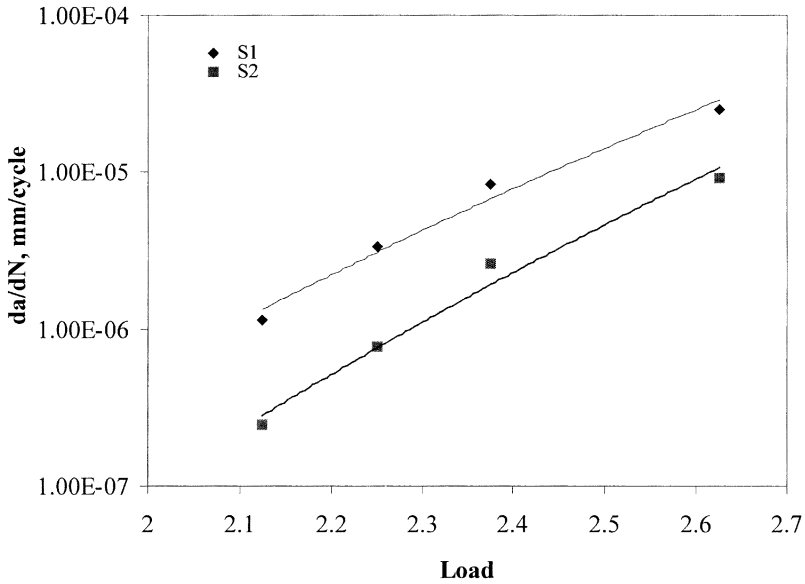

FIGURE 22 Plot of crack propagation rate with maximum fatigue load.

CONCLUSIONS

Backface strain provides a discriminating technique with which to quantify fatigue damage in bonded joints.

The backface strain technique has been studied using FE analysis for a wide range of joint and technique parameters. Experimental fatigue studies have validated the results of the FE analyses.

It has been shown that the sensitivity of the technique is optimal when the gauges are just within the overlap region and are as small as possible (subject to ease of installation).

Positioning the gauges in this way will result in the backface strain producing a clear peak as the damage evolves, and this is extremely useful as a benchmark when fatigue testing.

The sensitivity of the technique is greatest for more flexible substrates and decreases as they become stiffer.

Three different configurations of joints have been subjected to fatigue testing. Where these joints have been unmodified (no fillet removal) it would appear that even at the high load levels used there is a substantial period (about 50% of the total fatigue life) where little if any damage occurs. This could be thought of as the initiation period.

Removal of the adhesive fillet has been found to essentially eliminate the initiation phase of the fatigue life. This results in shorter fatigue lives and, hence, should be avoided.

It is likely, in view of the previously published work [7], that as this load level decreases the ratio of initiation to propagation periods will increase further.

Fatigue damage measured by microscopy on polished sections of partially tested joints correlates closely with damage predicted by FE analyses.

The backface strain technique has also been shown to provide an effective means of measuring (1) thresholds and (2) crack or damage propagation rates in bonded structures under fatigue.

REFERENCES

[1] Chang, B. H., Shi, Y. W. and Dong, S. J., *J. Matls. Proc. Tech.* **87**, 230–236 (1999).
[2] Crocombe, A. D. and Richardson, G., *Int. J. Adhes. and Adhesives* **19**, 19–27 (1999).
[3] Imanaka, M., Nakayama, H., Morikawa, K. and Nakamura, M., *Comp. Struct*, **31**, 235–241, (1995).
[4] Curley, A. J., Hadavinia, H., Kinloch, A. J. and Taylor, A. C., *Int. J. Fracture* **103**, 41–69 (2000).
[5] Xu, X. X., Crocombe, A. D. and Smith, P. A., *Intl. J. Fatigue* **16**, 469–477 (1994).
[6] Xu, X. X., Crocombe, A. D. and Smith, P. A., *Intl. J. Fatigue* **17**, 279–286 (1995).
[7] Johnson, W. S. and Mall, S., In: *Delamination and Debonding of Materials*, Johnson, W.S., Ed. ASTM STP 876 (ASTM, Philadelphia, 1975), pp. 189–199.

[8] Zhang, Z. and Shang, J. K., *J. Adhesion* **49**, 23–36 (1995).
[9] Abe, H. and Satoh, T., *J. Welding Soc. Japan* **10**, 272 (1992).
[10] Imanaka, M., Haraga, K., and Nishakawa, T., *J. Adhesion* **49**, 197–209 (1995).
[11] Lefebvre, D.R., Dillard, D.A. and Dillard, J.D., *J. Adhesion* **70**, 139–154 (1999).
[12] Crocombe, A.D., Yu, X.X. and Richardson, G., *J. Adhesion Sci. Technology* **15**, 279–302 (2001).
[13] Hart-Smith, L.J., Adhesives and Sealants, In: *Engineering Materials Handbook*, (ASM, Metals Park, Ohio, 1990), Vol. 3.
[14] Ashcroft I.A., Digby R.P. and Shaw S.J., *Proc. Joining and Repair of Plastics and Composites*, Instit. Mech. Eng. (London), March 1999, pp. 73–75.